Artificial phosphorylation sites modulate the activity of a voltage-gated potassium channel

Amila Ariyaratne and Giovanni Zocchi*

Department of Physics and Astronomy, University of California Los Angeles, Los Angeles, California 90095-1547, USA

(Received 8 September 2014; published 2 March 2015)

The KvAP potassium channel is representative of a family of voltage-gated ion channels where the membrane potential is sensed by a transmembrane helix containing several positively charged arginines. Previous work by Wang and Zocchi [A. Wang and G. Zocchi, PLoS ONE **6**, e18598 (2011)] showed how a negatively charged polyelectrolyte attached in proximity to the voltage sensing element can bias the opening probability of the channel. Here we introduce three phosphorylation sites at the same location and show that the response curve of the channel shifts by about 20 mV upon phosphorylation, while other characteristics such as the single-channel conductance are unaffected. In summary, we construct an artificial phosphorylation site which confers allosteric regulation to the channel.

DOI: 10.1103/PhysRevE.91.032701 PACS number(s): 87.16.Vy, 87.80.Jg, 87.50.cf

I. INTRODUCTION

Phosphorylation is the major post-translational modification of proteins [1]. It is well known that phosphorylation of proteins is a crucial component of regulatory networks in all living organisms. Mutations causing overphosphorylation or reduced phosphorylation often have dramatic effects. For example, familial advanced sleep phase syndrome is caused by a mutation in the hPer2 gene leading to a serine to glycine mutation in the casein kinase 1ϵ (CK1ϵ) binding region, which results in hypophosphorylation by CK1ϵ [2]. Phosphorylation also regulates the activity of voltage-dependent ion channels in neurons [3] and other cells. In humans, the potassium ion channel Kv11.1 is responsible for the action potential duration in ventricular myocytes (QT interval). The recently discovered K897T polymorphism [4] in this channel creates a new phosphorylation site for Akt, inhibiting the channel activity and thereby elongating the QT interval, which can be fatal. Thus, on the one hand, phosphorylation of ion channels is a physiologically important topic. On the other hand, from a bioengineering perspective, it is an interesting matter to construct artificial phosphorylation sites which confer allosteric modulation onto ion channels. This amounts to putting a given channel under the control of a user-defined kinase; the construction is genetically encoded and can, in principle, be transferred into the living neuron. These would be interesting tools for neuroscience research. The present work contributes to this second perspective.

Phosphorylation modulates the activity of voltage-dependent ion channels via electrostatic interactions with the voltage sensing domain [5]. Therefore, phosphorylation sites at different positions will affect the gating differently. Charge effects such as are seen by varying ionic conditions of the solution, bilayer composition, and the addition of charged amino acids to the sequence have been studied previously. For instance, Elinder and co-workers [6] used polyunsaturated fatty acids with charged groups to regulate an ion channel through electrostatic interactions with the voltage sensing domain. The trend observed is similar to what is reported here, in which negatively charged groups bias the Shaker K channel to the hyperpolarizing direction. We previously studied the effect on gating caused by the addition of charges near the voltage sensing domain of KvAP, using ion channel-DNA chimeras [7]. Wang *et al.* constructed KvAP channels with a single strand of DNA attached to the pore domain and found that the added negative charge shifts the gating behavior towards inhibition. Hybridization of the single stranded DNA with the complementary strand could reverse the inhibition by shifting the DNA charge away from the voltage sensing domain. In this study, we create an artificial phosphorylation site on the voltage-gated potassium channel KvAP at the position where the single stranded DNA was attached in the study of Wang *et al.* We add a seven amino acid sequence (PATPTPT) that creates a threonine phosphorylation site (Fig. 1) for the mitogen activated protein kinase (MAPK) and measure the effect on gating. We find that phosphorylation of this artificial site does indeed shift the opening probability vs voltage curve, i.e., the gating behavior of the channel, by about 20 mV towards inhibition. This is our main (indeed, only) result: we were able to construct an artificial phosphorylation site for this particular channel which confers (limited) allosteric modulation to the channel upon phosphorylation. We note in passing that this behavior is consistent with the expected electrostatic coupling between the added charges and the voltage sensing domain, and is consistent with the interpretation given in Wang *et al.* of the effect of the DNA charges at the same location. Indeed, these simple electrostatic considerations were the rationale for the choice of location for the phosphorylation site, though this coincidence of design and result may, of course, be fortuitous.

KvAP is a voltage-gated potassium channel from *Aeropyrum pernix*. Ruta *et al.* characterized the KvAP channel functionally [8] and found that it has a conductance of $\sim$170 pS; the channel undergoes inactivation similar to other Kv channels and pore blocking toxins bind to block KvAP in a similar manner to other Kv channels. The structure of KvAP was solved in 2003 by the MacKinnon laboratory [9]. It is a tetramer, with each unit comprising a voltage sensing domain (VSD) and pore forming domain. The central pore domain is the ion conduction pathway (Fig. 2). The S4 helix of the VSD contains five arginine amino acid groups which are positively charged; four of these contribute to

*zocchi@physics.ucla.edu

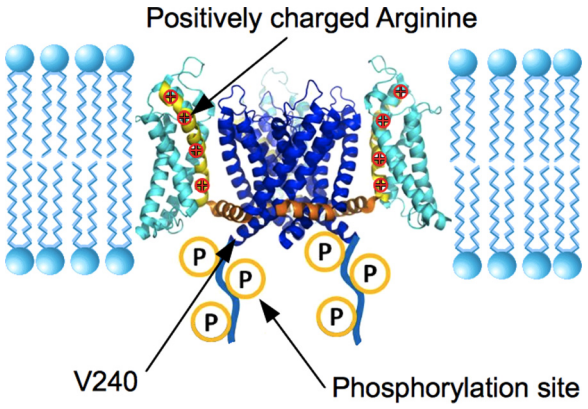

FIG. 1. (Color online) Location of the artificial phosphorylation sites on the KvAP ion channel. The ion channel structure shown is that of a Kv channel with a similar structure to that of KvAP (Mammalian Shaker Kv 1.2, PDB ID: 2A79). The seven amino acid sequence containing the phosphorylation sites is added after the site valine 240, as shown in the figure. The three phosphorylation sites are denoted by the circled letter P's. For clarity, only two of the four monomers are shown with the phosphorylation modification.

voltage-dependent gating [8]. It is well established that these arginines move in response to the electric field across the membrane [10,11].

Here we added a seven amino acid sequence to the KvAP gene in order to create a phosphorylation site on it. This sequence was determined using the web-based application KINASEPHOS [12]. The KINASEPHOS web application is based on a profile hidden Markov model (HMM) to predict the phosphorylation sites on a protein. We found that this web application predicted the sequence PATPTPT to have three threonine phosphorylation sites catalyzed by the kinase MAPK when inserted between the positions V240 and G241 of the KvAP protein monomer. The prediction specificity for the above three sites was 100%. Further, the wild-type KvAP did not have any phosphorylation sites for the kinase MAPK. Figure 1 illustrates how the phosphorylation sites might be present when the channel is functional in a lipid bilayer. In the study of Wang *et al.*, the DNA was coupled to the residue valine 240 (which was mutated to a cysteine).

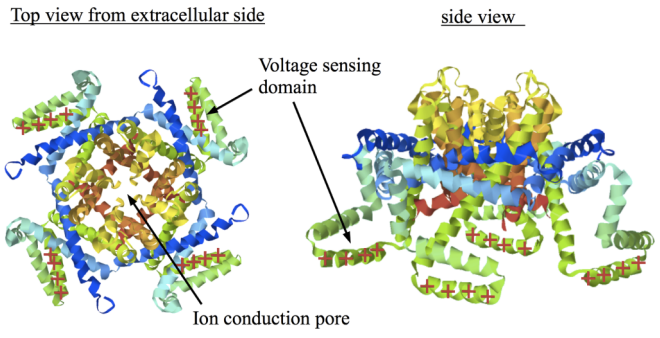

FIG. 2. (Color online) Structure of the KvAP ion channel (PDB 1ORQ). The functional channel is a tetramer with the central pore domain forming the ion conduction pathway. Red + signs indicate the positively charged arginine amino acids involved in gating.

II. MATERIALS AND METHODS

A. Mutagenesis of KvAP gene

The cloned gene of the voltage-dependent K+ channel from *Aeropyrum pernix* in the vector pQE60 was obtained as a gift from Mackinnon (The Rockefeller University). Site directed mutagenesis (QuickChange, Agilent Technologies) was used to remove the native cysteine at the sequence site 247 to a serine which does not change channel functionality. The artificial phosphorylation site comprising the seven amino acids sequence PATPTPT was added to the KvAP gene between the sequence sites valine 240 and glycine 241 by using the DNA sequence 5′-CCTGCCACCCCTACCCCTACC-3′. All mutants were confirmed by gene sequencing performed by the UCLA GenoSeq Laboratory. After glycine 241, the gene contains an unstructured, intracellular, 40 amino acids long part ending in the C terminus.

B. Expression and purification of KvAP protein

The KvAP gene in the expression vector pQE60 was expressed in *E. coli* cells (Agilent Technologies XL1-Blue). Transformation of the plasmid vector into the cells was achieved by giving a heat pulse of 42 °C for a duration of 45 s. All of the procedures below were performed at room temperature, and were adapted from [8]. The protein expressed in 10 g of *E. coli* was resuspended in 50 mL of lysis buffer (50 mM Tris at pH 8.0, 100 mM KCl, 0.2 mg/mL lysozyme, 2 μg/mL DNase, 2 mM beta-ME and protease inhibitor cocktail) and lysed using a French Press. Decylmaltoside detergent at 40 mM (DM, Anatrace) was used for three hours to extract the channel protein from the lysate. The supernatant obtained by centrifuging the lysate-DM mixture was passed through a Talon affinity column (Clontech) so the His-tagged ion channel binds to the beads. Before adding the protein supernatant, the Talon beads were washed with 30 mL of wash buffer (20 mM Tris at pH 8.0, 100 mM KCl, 10 mM imidazole, and 5 mM DM). Then the bead-supernatant mixture was gently rotated for one hour and subsequently was passed through the column four times to retain all the beads in the column. Wash buffer (30 mL) was used to remove nonspecifically bound species from the beads followed by 10 mL of elution buffer (similar to wash buffer but with 400 mM imidazole) to elute the ion channel. 1.5 units of thrombin (Sigma) were added to each mg of channel protein to cleave the His-tag overnight. The protein treated with thrombin was run in a size exclusion Superdex-200 column (GE Healthcare) in a high-performance liquid chromatography (HPLC) buffer (20 mM Tris at pH 7.5, 100 mM KCL and 5 mM DM).

C. Phosphorylation of the KvAP protein

Phosphorylation of the threonine phosphorylation sites was achieved using the p42 MAP kinase (mitogen-activated protein kinase, MAPK, New England Biolabs Inc.). The ion channel protein purified with size exclusion chromatography (in the HPLC buffer) was treated with 5 units of MAPK, 10 mM MgCl2, and 1 mM adenosine triphosphate (ATP) and was incubated at 30 degrees for three hours. After the incubation period, the ion channels were purified using size exclusion chromatography (Sephadex 200 column) to remove ATP, adenosine

diphosphate (ADP), MgCl2, and MAPK, etc. Sodium dodecyl sulfate–polyacrylamide gel electrophoresis (SDS-PAGE) was performed on HPLC purified KvAP protein samples before and after phosphorylation (in the same gel). We had difficulty in running a native PAGE on the ion channel protein; instead, we used a modified SDS-PAGE in which the standard SDS concentration was reduced by a factor of 100. However, in the end, it was not clear that this procedure leads to improved resolution (as far as distinguishing phosphorylated from unphosphorylated proteins) compared to standard SDS-PAGE.

D. Measuring the phosphorylation of KvAP ion channels

Spectroscopic measurements were made on a Beckmann Coulter DTX800 Multimode Detector. Enzyme activity measurements are based on a coupled enzyme assay [13], which involves three coupled reactions: production of ADP from ATP (phosphoryl transfer), pyruvate kinase reaction where ADP reacts with phosphoenolpyruvate (PEP) to yield ATP and pyruvate, and lactate dehydrogenase reaction where the pyruvate participates in the catalytic oxidization of nicotinamide adenine dinucleotide reduced (NADH) to nicotinamide adenine dinucleotide (NAD+). The consumption of ATP is therefore monitored by the decrease of NADH measured as the decrease in fluorescence at 465 nm. For each measurement, the reaction mixture consisted of 50 uL of the HPLC purified KvAP ion channels before the phosphorylation (in HPLC buffer), 100 mM MgCl2, 150 uM NADH, 0.5 mg/ml Bovine Serum Albumin (BSA), 100 mM PEP, 10 units/ml pyruvate kinase, 13.2 units/ml lactate dehydrogenase, and 5 units of MAPK. ATP was added to the reaction to a concentration of 5 mM just before taking the fluorescence measurements.

E. Reconstitution of KvAP ion channel into lipid vesicles

The lipid DphPC (Avanti) was used to make vesicles; the procedure below is adapted from [14]. First the lipid in chloroform was dried using a pure nitrogen flow, followed by adding $\sim$250 μL pentene and drying. The dried lipid was then put under a vacuum for one hour before dissolving in reconstitution buffer (10 mM HEPES-KOH at pH 7.4 and 450 mM KCl) for a lipid concentration of 20 mg/mL obtained by rapid vortexing for 30 minutes. The resulting lipid solution was then sonicated for 20–30 minutes to form unilamellar vesicles and was dissolved in 10 mM DM for 30 minutes. The concentrated ion channel protein ($\sim$4 mg/mL) was then added to the lipid vesicle solution, to a lipid to protein ratio of 1 (wt/wt). The detergent concentration was then raised to 17.5 mM and the mixture was incubated for two hours with gentle vortexing every 20 minutes. The next phase of reconstitution is to remove the DM. First the vesicle-protein solution is passed through three spin desalting columns (Pierce). Then an adequate amount of detergent absorbing biobeads (Bio-Rad) which were washed prior to use (first in methanol, then in deionized water, and finally in reconstitution buffer) were added to the vesicle-protein solution, which was kept at 4 °C. The biobead procedure was repeated every 12 hours for another three times. At the end of the fourth cycle, the detergent free protein vesicles were flash frozen (using an ethanol–dry ice bath) in small aliquots and stored at −80 °C for later use.

F. Electrophysiology setup

A planar lipid bilayer setup was used to measure the activity of the ion channels as we have described previously [7]. The melt and shave method described in Wonderlin *et al.* [15] was used to make a cone-shaped dent in a plastic Ultra-Clear™ (Beckman Coulter) tube. Then the dent was shaved with a sharp blade to obtain a $\sim$150 μm circular aperture and was fixed to a Teflon holder which served as the extracellular chamber (trans chamber). The whole system was then mounted on an inverted microscope so that the bilayer formation could be viewed (8).

DPhPC lipid was taken fresh from the −80 °C freezer for each experimental run and was dried according to the method mentioned above. n-Decane was added to the dried lipid to a lipid concentration of 20 mg/ml. Then a small drop of lipid ($<$0.5 μL) was put on to the aperture and was allowed to dry. The two chambers were then filled with a buffer containing 150 mM KCl, 10 mM HEPES-KOH at pH 7.4, and a second small drop of lipid was added. The removal of excess lipid from the aperture using a small glass spatula resulted in the formation of a bilayer. Once a stable bilayer was available, a dose of channel vesicles was added to the cis chamber from a fresh aliquot of channel vesicles (thawed and sonicated for $\sim$10 s). Vesicle fusion to the bilayer could be seen as spiking events when the holding voltage was kept at −120 mV and the process was accelerated by stirring the cis chamber with a glass rod.

Ion channel currents were detected using a home-built voltage-clamp amplifier with a feedback resistor of 22 MΩ. The output from the voltage-clamp amplifier was fed into a low noise preamplifier (SR560, Stanford Research Systems). The signal was digitized using an analog to digital converter (NI USB-6009, National Instruments) and recorded using the software LABVIEW SIGNAL EXPRESS (National Instruments). A battery powered pulse generating circuit was used to generate the voltage protocol across the bilayer.

III. RESULTS

A. Comparison of wild-type and modified channels

The modified ion channel protein, i.e., with the PATPTPT insertion, was functional and showed a single-channel conductance similar to the wild-type KvAP channel. Figure 3(a) shows a single-channel current trace of a KvAP ion channel with the phosphorylation sequence added, but not phosphorylated, elicited with a 60 mV voltage step. Different depolarizing potentials were given to these channels and the single-channel conductance was found to be 170 pS under symmetric salt conditions of 150 mM KCl, identical to the wild-type conductance. Figure 3(b) shows the multichannel current trace from the same channels. The current trace was obtained by using a voltage step of 60 mV. The initial fast rise of the current corresponds to the stochastic opening of the channels, while the later slow decay corresponds to the well-known inactivation of the channels after a prolonged depolarization pulse. This inactivation time scale was found to be 135 ms for the modified KvAP channel (Fig. 4), whereas the inactivation time scale of the wild-type KvAP is about 400 ms [16]. Figure 5 shows the open probability curve for these channels, obtained by applying different depolarizing

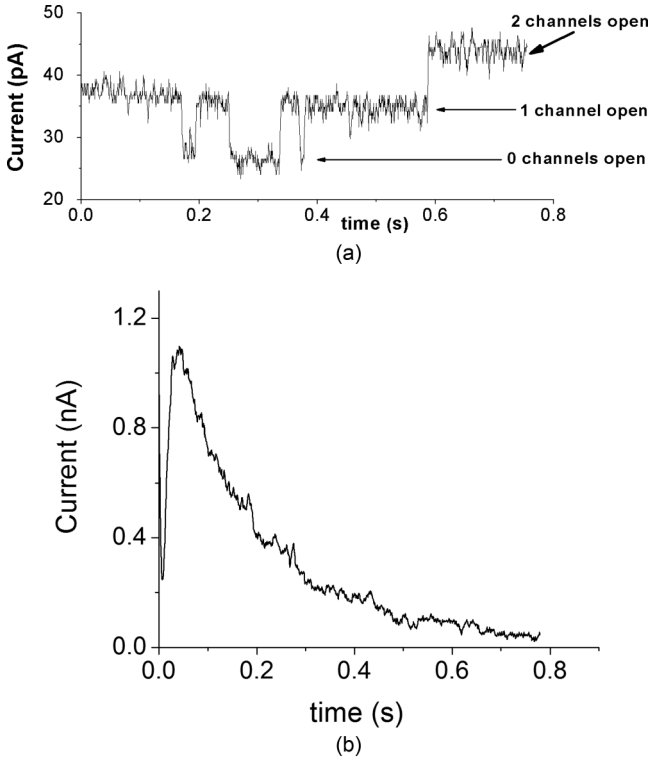

FIG. 3. Current traces of the modified KvAP ion channels before phosphorylation, obtained by depolarizing the channels to 60 mV after holding the channels at the hyperpolarizing potential of −120 mV for 10.8 s. Here, as in rest of the paper, the electrophysiological recordings were obtained with symmetric salt conditions of 150 mM KCl. (a) A single-channel current trace. (b) Multichannel current trace of the unphosphorylated ion channels corresponding to about 100 channels. The initial fast rise is due to the stochastic opening of the channels, whereas the exponential decay at longer times is due to inactivation of the channels.

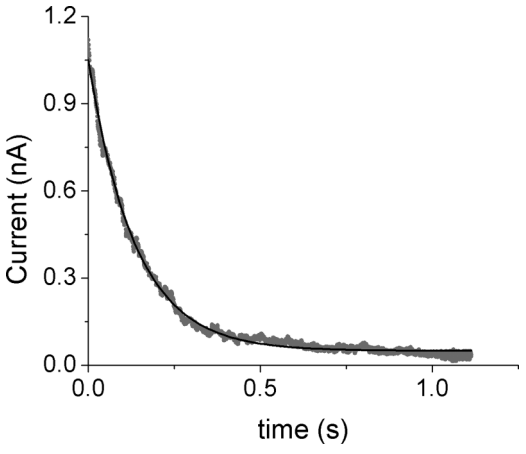

FIG. 4. Inactivation time scale of unphosphorylated KvAP mutant. The current trace shown in gray is the average of five traces obtained by depolarizing the channels with a 60 mV step and the portion of the trace which corresponds to inactivation was used to determine the inactivation time scale. The black curve was obtained by fitting data to an equation of the form $I = I_0 \exp(-t/\tau) + I_{\text{background}}$, which gave $\tau = 135$ ms.

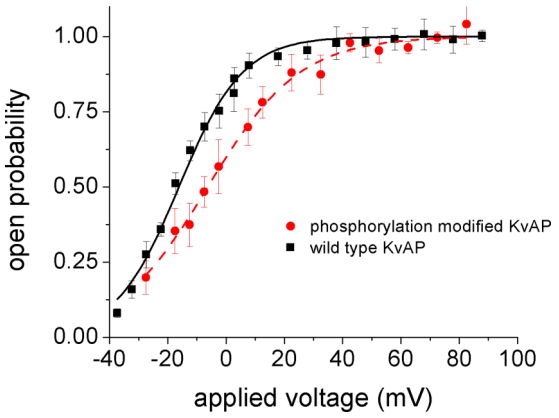

FIG. 5. (Color online) Dependence of the open probability (the fraction of time the channel is open) on the membrane voltage. The black squares correspond to the wild-type KvAP, while the red circles correspond to the modified KvAP (with the phosphorylation sites inserted but not phosphorylated). The open probability vs voltage V is measured from the peak current I_0 obtained by depolarizing the channels with a voltage step ending at V. The conductance I_0/V, plotted vs V, and normalized to 1 at high V, is shown in the figure. The data for each curve is from the same bilayer. Each point is the average of five readings and the error bars show the standard deviation. We obtained essentially identical curves from several different independent bilayers. It can be observed that the addition of the extra amino acid sequence results in a change of the open probability curve towards more positive voltages, implying that the modified channel needs a higher depolarizing voltage than the wild type to have the same open probability.

voltage steps. Compared to the wild type (also shown in Fig. 5), the curve is less steep and shifted to higher voltage. This is reflected in the parameters of the fits shown in the figure: $E = 37.9$ meV $= 1.48$ kT, $\alpha = 2.34$ for the wild type and $E = 9.98$ meV $= 0.39$ kT, $\alpha = 1.62$ for the modified channel [see Eq. (4)].

B. Phosphorylation of the channel

The phosphorylation of the modified KvAP was measured by the assay introduced by Agarwal *et al.* [13], in which the reaction of phosphoryl transfer, here between adenosine triphosphate (ATP) and the amino acid threonine catalyzed by MAPK, is coupled to two downstream reactions:

$$\text{ATP} + \text{threonine} \overset{\text{MAPK}}{\rightleftharpoons} \text{ADP} + \text{phosphorylated threonine} \tag{1}$$

$$\text{ADP} + \text{PEP} \overset{\text{PK}}{\rightleftharpoons} \text{ATP} + \text{pyruvate} \tag{2}$$

$$2\,\text{pyruvate} + 2\text{NADH} \overset{\text{LDH}}{\rightleftharpoons} 2\text{lactate} + 2NAD +, \tag{3}$$

where PK is the pyruvate kinase, catalyzing phosphoryl transfer from phosphoenolpyruvate (PEP) to ADP and production of pyruvate; LDH is lactate dehydrogenase catalyzing the interconversion of pyruvate and lactate with the concomitant interconversion of NADH and NAD+. The final reading of the

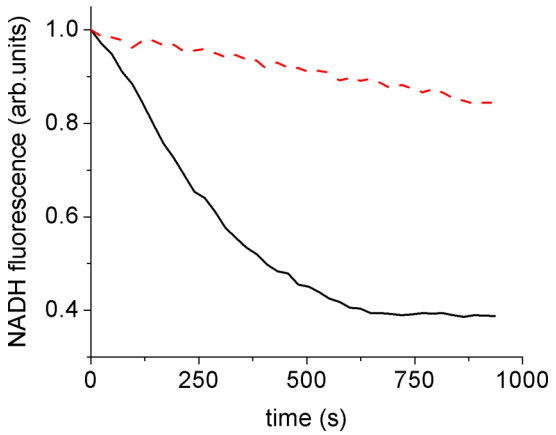

FIG. 6. (Color online) Assay for the phosphorylation of the KvAP (see Sec. II). NADH fluorescence vs time for the wild-type (dashed curve) and modified (solid curve) KvAP, under phosphorylating conditions. The phosphorylation reaction converts ATP to ADP; the ADP produced is coupled to the consumption of NADH which is fluorescent at 465 nm. Thus, as phosphorylation of the modified KvAP proceeds, NADH fluorescence decreases (solid curve). The dashed curve is the control with the wild-type KvAP; the linear decrease, corresponding to the background ATP hydrolysis, is much weaker compared to the phosphorylation signal. The kinase used for phosphorylation in this paper is MAPK.

activity measurement is the decreasing fluorescence of NADH at 465 nm (excitation at 365 nm). As a control, phosphorylation of the wild-type KvAP by MAPK kinase was tested along with phosphorylation of the KvAP channel with the phosphorylation site insertion. Figure 6 shows the fluorescence of NADH measured for the phosphorylation reaction of KvAP in the unmodified and modified forms. The phosphorylation reaction was performed on ion channels dissolved in 5 mM detergent (decylmaltoside). Each phosphorylation reaction contained 5 units of MAPK, 20 μM ATP, and 20 mM $MgCl_2$. It can be observed that the NADH reaction proceeds only with the modified KvAP. From the data of Fig. 6, we estimate that 5 units of MAPK in our reaction mixture transfers $\sim$500 pmol of phosphate groups from ATP to the modified KvAP in $\sim$10 minutes. This is comparable (within a factor 10) to the nominal speed from the vendor (New England Biolabs murine p42 MAPK).

SDS-PAGE was performed after incubating the KvAP modified protein with the MAPK enzyme for one hour to observe mobility differences in the gel due the added charges. Figure 7(a) shows the SDS-PAGE result for the modified KvAP before and after phosphorylation. We see from the gel a slight increase in mobility after phosphorylation, consistent with the fact that phosphorylation introduces more negative charges on the protein. It must be mentioned that native PAGE is ideally the better assay for this situation since the mobility is then dependent only on the charge of the protein, which changes considerably upon phosphorylation. However, a few trials at a native PAGE with the KvAP were unsuccessful. Instead, we found that a modified PAGE, where we reduced the amount of SDS by 100 times compared to the standard, also produced results. Figure 7(b) shows this modified gel of the KvAP before and after phosphorylation, where again

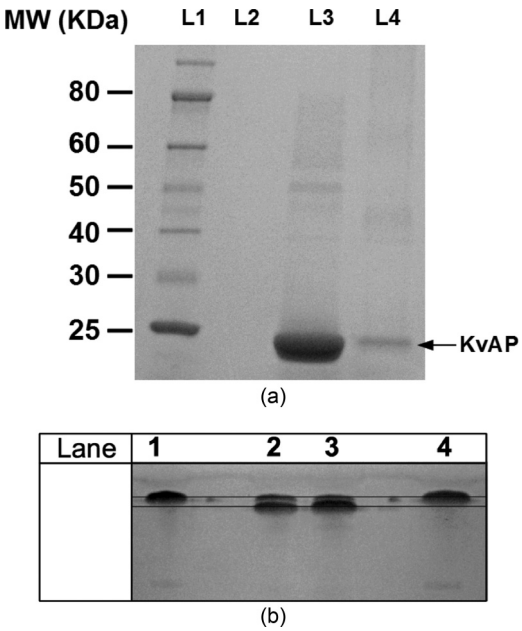

FIG. 7. SDS-PAGE to observe phosphorylation of the modified KvAP ion channel. (a) Lane 4 shows the modified KvAP ion channel before treating with MAPK, while Lane 3 is the modified KvAP after incubating with MAPK for three hours. Lane 3 had more samples than Lane 4. The slightly higher mobility of the phosphorylated KvAP sample (Lane 3) is consistent with the ion channel being more negatively charged than the unphosphorylated KvAP (Lane 4). (b) Modified SDS-PAGE in which the SDS concentration was reduced by a factor of 100 compared to the standard. Lanes 1 and 4 correspond to the unphosphorylated ion channel, while Lanes 2 and 3 are the phosphorylated channel. The added charge due to phosphorylation results in a slight increase in mobility.

we observe a slight increase in mobility with a more sharply defined band. From the gels, we see that a majority of the monomers are phosphorylated; therefore, in the reconstituted channels, typically three or four out of the four subunits will be phosphorylated. We also think it unlikely that, in the monomer, more than one out of three phosphorylation sites is phosphorylated because of the proximity of the sites. Taken together, the likely scenario is that typically, in the phosphorylated channels, there is one phosphate group per subunit. However, we have not directly measured this number.

C. Electrophysiology of the phosphorylated KvAP

The modified KvAP ion channels were incubated with MAPK overnight after purification (in 5 mM DM) and were reconstituted into lipid vesicles as described in Sec. II. These channels were incorporated into planar lipid bilayers (Fig. 8) to study their electrophysiological properties. Figure 9 shows a single-channel current trace from these phosphorylated channels. The channels were depolarized to a voltage of 60 mV after resting in the hyperpolarized voltage of -120 mV. Different depolarizing voltages were applied to determine the single-channel conductance and it was found that the conductance remained unchanged at 170 pS.

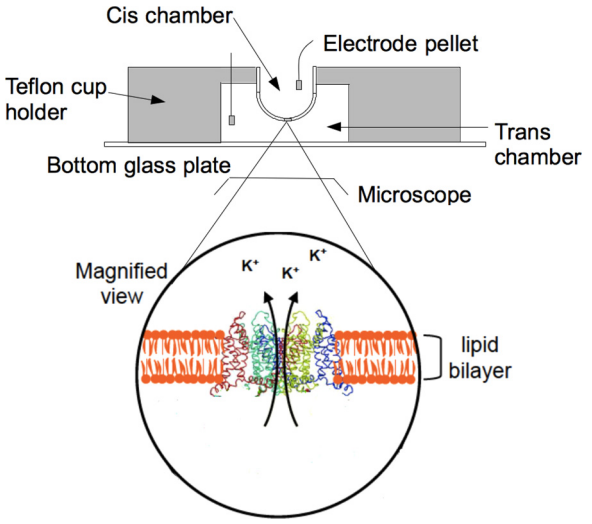

FIG. 8. (Color online) The planar lipid bilayer system. The artificial bilayer is stretched across a ∼100 μm hole crafted in a plastic test tube mounted on a Teflon holder. Electrical connections to the bilayer chamber were made via Ag/AgCl electrodes. The whole system is mounted onto the x-y stage of an inverted microscope.

Multichannel recordings of the phosphorylated KvAP were studied to determine the effect on gating caused by the addition of the negative charges from phosphorylation. The inactivation time scale of the modified KvAP dropped from 135 ms to about 90 ms after phosphorylation. Figure 10 shows the open probability curve for the phosphorylated and unphosphorylated channels. Phosphorylation causes a ∼20 mV shift of the opening probability curve towards higher voltages.

IV. DISCUSSION

The insertion of a seven residue tract containing three phosphorylation sites on the intracellular side of the channel (Fig. 1) did not disrupt the working of the channel and, in particular, did not alter the single-channel conductance. The modification did cause a change in the opening probability curve (Fig. 5), and also a change in the characteristic time scale for inactivation. Phosphorylation of the modified channel shifts the opening probability curve to higher voltage, while

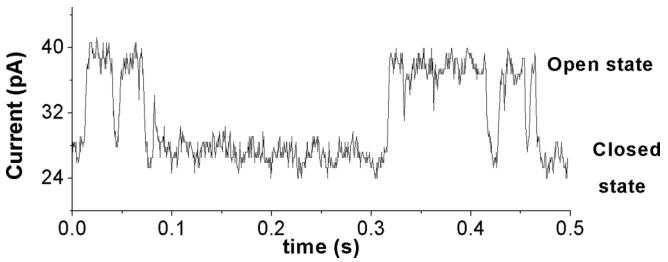

FIG. 9. Single-channel current trace of the modified KvAP ion channels after phosphorylation, obtained by depolarizing the channels to 60 mV after holding the channels at the hyperpolarizing potential of −120 mV for 10.8 s. From these current traces, we found that the single-channel conductance is unaffected by phosphorylation of the channel.

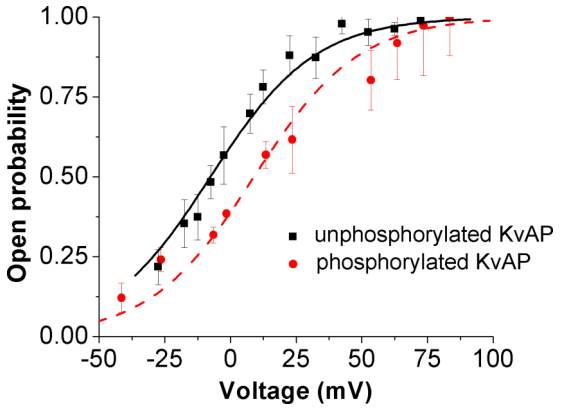

FIG. 10. (Color online) Dependence of the opening probability (the fraction of time the channel is open) on the membrane voltage for the modified KvAP ion channels before and after phosphorylation. The red dots indicate the phosphorylated ion channels, while the black squares are from the unphosphorylated ion channels (this is the same data set as the red dots in Fig. 5). The effect of phosphorylation is to inhibit the channels by translating the opening probability curve towards more positive voltages. The data for each curve are from the same bilayer. Each point is the average of five readings and the error bars show the standard deviation. We obtained essentially identical curves from two different independent bilayers for the phosphorylated case and several independent bilayers for the unphosphorylated case. The lines are fits with Eqs. (4) and (5).

also leaving the single-channel conductance unaffected. Thus we can say that the charges added by phosphorylation interact with the voltage sensor movement but not with the conduction process of ions flowing through the pore. All in all, we demonstrate inhibition of channel activity by an artificial phosphorylation site. However, we also note that the conditions of the measurement are quite artificial compared to the live cell situation. We use symmetric salt conditions, and potassium only. Also, the artificial membrane is quite different from a real cell membrane in terms of composition. Thus there is no guarantee that the results will carry over unchanged for the channels in the live cell. The question of how asymmetric ionic conditions similar to those for real cell membranes would affect the results seems particularly relevant, as pointed out by one referee, and we hope to address it in further studies with this system.

Another comment is that this study was motivated, for us, by the general concept of modulating the activity of biological macromolecules by exerting forces, in this case the electrostatic force from an extra charge delivered by phosphorylation. From this point of view, we expect any force field or perturbation which adds a stress on the molecule to have some effect on the opening probability curve. Indeed, Fig. 5 shows the effect of merely adding seven (uncharged) residues to the unstructured coil after V240. One would expect this perturbation to cause a relatively minor change in the osmotic stresses on the molecule, but in the end the effect on the opening probability curve is surprisingly of the same magnitude as the effect of phosphorylation. The conclusion is that the response of the channel can, in principle, be modulated artificially in many different ways; the bioengineering problem is, of course, to find effective and useful ways.

Now we show that the simplest model (by no means original) where electrostatic interactions bias the gating is qualitatively consistent with the measured effect of phosphorylation as shown in Fig. 10. More detailed models of electrostatic interactions in ion channels have been considered before. For example, Elinder and co-workers [17] calculated the electrostatic potential at the voltage sensing domain due to the charged residues in the S5-P loop of voltage-gated potassium channels using the Grahame equation for the surface charge. For us, the electrostatic interaction in question is between a negatively charged phosphate at the position shown in Fig. 1 and the positively charged arginines on the S4 helix. The voltage sensor comprises the S4 helix, which has four positively charged arginine residues that are responsible for the gating process [8]. These arginines move in response to the transmembrane electric field [18]. Adding a negative charge at the position of the phosphorylation sites shown in Fig. 1 pulls the S4 helix downwards in the figure, biasing the channel towards the closed conformation. The effect of the added phosphate is similar to the effect of a negative biasing voltage. The distance from the position V240 to the middle of the S4 helix (in the closed structure) is about 3 nm. The Debye screening length in the salt solution is $\sim$1 nm; the dielectric constants for water and the protein are, respectively, $\epsilon_1 = 80$ and $\epsilon_2 = 2$. To estimate the electrostatic interaction energy between the added phosphate group and the S4 helix, we invoke the following simplified geometry: charges $Q_p = -2|e|$ (the phosphate) and $Q_a = +2|e|$ (the two nearest arginines) separated by an average distance $R = 3$ nm; e is the electronic charge. For two charges located on the same that are normal to, and opposite sides of, a plane interface between dielectrics 1 and 2, the effective dielectric constant for the purpose of calculating the electrostatic energy is $\epsilon_{\rm eff} = (\epsilon_1 + \epsilon_2)/2$, independent of the position of the interface [19]. The estimate for the electrostatic energy W is, therefore, $W \approx (Q_p Q_a)/(\epsilon_{\rm eff} R) \approx (4e^2)/(40 \times 3 \ \ {\rm nm})$ or $W \approx 4 \times (4.8 \times 10^{-10}\ {\rm esu})^2/(40 \times 3 \times 10^{-7}\ {\rm cm}) \approx 10^{-13}$ ergs ≈ 50 meV $\approx 2\,kT$. On the other hand, we can obtain the actual electrostatic energy directly from the measurements. We assume a two-state model for the opening probability of the channel,

$$P(V) = \frac{1}{1 + e^{-(E+\alpha|e|V)/kT}}, \tag{4}$$

where E is the energy difference between the two levels at zero applied voltage and α is a dimensionless number which gives the steepness of the response curve. The addition of a charge in proximity to the voltage sensing domain can be thought of as adding a negative energy term to E in the above equation. Then, the opening probability after phosphorylation is

$$P_p(V) = \frac{1}{1 + e^{-(E-\Delta+\alpha|e|V)/kT}}, \tag{5}$$

where Δ is the electrostatic energy in question. The experimental value of Δ can be determined by fitting the opening probability curves before and after phosphorylation. From the fits in Fig. 10, we find $E = 0.38\,kT$ and $\Delta = 0.8\,kT$, while $\alpha = 1.28$. Thus the measured displacement of the opening probability curve ($\Delta V = 17$ mV) is about half what we obtain from the model (5) using the estimated Coulomb energy of the charges [$2\,kT/(\alpha|e|) = 38$ mV]. Since $1\,kT \approx 25$ meV, in this description each kT of electrostatic energy shifts the curve by 25 mV/$\alpha \approx 19$ mV.

The foregoing discussion evidently does not prove that the effect shown in Fig. 10 is predominantly due to electrostatic attraction between the charged phosphate and the arginines on the S4 helix. Obviously, the charged phosphate also interacts with all other charges and dipoles in the molecule and the bilayer. The electrostatic energy estimated from the geometry, $\Delta \approx 2\,kT$, has the right sign and order of magnitude when we compare it, using (5), to the shift in the opening probability curve reported in Fig. 10. However, there is a numerical discrepancy of more than a factor of 2; either the model (5) is too simple or the estimate for Δ is too crude, or both. In addition, there are other effects of adding charges, besides direct electrostatic interactions between charged residues. An important part is probably played by excluded volume (osmotic pressure) interactions. Figure 5 shows that an effect on the open probability curve of similar magnitude as the effect in Fig. 10 is obtained by adding a seven amino acid tract after V240 (Fig. 1). The 40 amino acid "tail" after V240 is unstructured and forms, presumably, a polymer coil dangling off the intracellular side of the channel. Due to excluded volume interactions, the presence of this coil must produce a stress on the channel, which depends on the length of the coil. Such effects could be at the origin of the change in the opening probability curve seen in Fig. 5, so obviously they are important. Note, however, that the changes in the opening probability curve of Fig. 10 appear to be a simple shift along the voltage axis, different from the changes in Fig. 5. All in all, the simple electrostatic reasoning of this section may predict the sign but not the magnitude of the effect of phosphorylation. This statement can be tested experimentally; for example, Hyperpolarization-activated cyclic nucleotide-gated (HCN) channels have a similar architecture with gating based on the motion of the positively charged S4 helix, but the action is reversed (pulling the helix towards the intracellular side opens the channel) [20]. Will phosphorylation at a site homologous to the site of the present study shift gating in the direction of activation in this case?

In summary, we have introduced an artificial phosphorylation site on the KvAP channel and have shown that phosphorylation of this site shifts gating by approximately 20 mV in the direction of inhibition. To place this work in a more general context, we remark that tuning the dynamic range of response of molecular sensors through mutagenesis and allosteric regulation is currently an active area of research [21], with ramifications in synthetic biology. On the other hand, the recent development of optogenetics [22–25] demonstrates that the engineering of artificial control elements specifically on ion channels [25–27] may result in useful new tools for neuroscience research.

[1] L. N. Johnson, Biochem. Soc. Trans. **37**, 627 (2009).
[2] K. L. Toh *et al.*, Science **291**, 1040 (2001).
[3] D. A. Fadool, T. C. Holmes, K. Berman, D. Dagan, and I. B. Levitan, J. Neurophysiol. **78**, 1563 (1997).

[4] S. Gentile, N. Martin, E. Scappini, J. Williams, C. Erxleben, and D. Armstrong, Proc. Natl. Acad. Sci. USA **105**, 14704 (2008).
[5] E. P. F. Bezanilla, Neuron **5**, 685 (1990).
[6] S. Börjesson, T. Parkkari, S. Hammarström, and F. Elinder, Biophys. J. **98**, 396 (2010).
[7] A. Wang and G. Zocchi, PLoS ONE **6**, e18598 (2011).
[8] V. Ruta, Y. Jiang, A. Lee, J. Chen, and R. MacKinnon, Nature (London) **422**, 180 (2003).
[9] S.-Y. Lee, A. Lee, J. Chen, and R. MacKinnon, Nature (London) **102**, 15441 (2005).
[10] D. Posson, P. Ge, C. Miller, F. Bezanilla, and P. Selvin, Nature (London) **436**, 848 (2005).
[11] G. Yellen, Quar. Rev. Biophys. **31**, 239 (1998).
[12] H.-D. Huang, T.-Y. Lee, S.-W. Tzeng, and J.-T. Horng, Nucleic Acids Res. **33**, W226 (2005).
[13] R. P. Agarwal, K. C. Miech, and R. Parks, Methods Enzymol. **51**, 483 (1978).
[14] L. Heginbotham, M. LeMasurier, L. Kolmakova-Partensky, and C. Miller, J. Gen. Physiol. **114**, 551 (1999).
[15] W. Wonderlin, A. Finkel, and R. French, Biophys J. **58**, 289 (1990).
[16] P. Devaraneni, A. Komarov, C. Costantino, J. Devereaux, K. Matulef, and F. Valiyaveetil, Proc. Natl. Acad. Sci. USA **110**, 15698 (2013).
[17] F. Elinder and P. Århem, Biophys. J. **77**, 1358 (1999).
[18] B. Chanda, O. K. Asamoa, R. Blunck, B. Roux, and F. Bezanilla, Nature (London) **436**, 852 (2005).
[19] J. Jackson, *Classical Electrodynamics* 3rd ed. (Wiley, New York, 1998).
[20] C. Wahl-Schott and M. Biel, Cell. Mol. Life Sci. **66**, 470 (2009).
[21] A. Porchetta, A. Vallee-Belisle, K. W. Plaxco, and F. Ricci, J. Am. Chem. Soc. **134**, 20601 (2012).
[22] M. Banghart, K. Borges, E. Isacoff, D. Trauner, and R. Kramer, Nat. Neurosci. **7**, 1381 (2004).
[23] E. S. Boyden, F. Zhang, E. Bamberg, G. Nagel, and K. Deisseroth, Nat. Neurosci. **8**, 1263 (2005).
[24] L. Fenno, O. Yizhar, and K. Deisseroth, Annu. Rev. Neurosci. **34**, 389 (2011).
[25] J. Chambers, M. Banghart, D. Trauner, and R. Kramer, J. Neurophysiol. **96**, 2792 (2006).
[26] U. Ohndorf and R. MacKinnon, J. Mol. Biol. **350**, 857 (2005).
[27] A. Kocer, M. Walko, W. Meijberg, and B. Feringa, Science **309**, 755 (2005).